Proceedings of Australasian Conference on Robotics and Automation, 2-4 Dec 2014, The University of Melbourne, Melbourne, Australia

Rotor Flapping for a Triangular Quadrotor

Jaco du Plessis and Paul E. I. Pounds*
University of Queensland, Australia
jaco.duplessis@uqconnect.edu.au, paul.pounds@uq.edu.au

Abstract

The triangular quadrotor is a novel, more efficient configuration of quadrotor aircraft that uses a single large central rotor for lift and three smaller rotors for counter-torque and manoeuvering. Early experiments exhibited a precession effect due to the uncompensated gyroscopics of the main rotor. In this paper we discuss two techniques to fix this problem: feedback linearisation and a mechanical flapping joint. Simulations indicate that, contrary to expectations, feedback linearisation is not viable due to delays in the control system. The rotor flapping approach is shown to be a more effective solution, both in simulation and flight experiments.

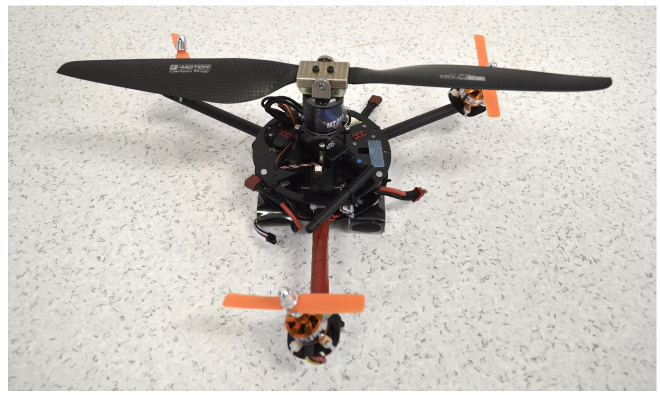

Figure 1: Triangular Quadrotor with Flapping Hinge.

1 Introduction

Increasing demands for improved flight time and payload of Unmanned Aerial Vehicles (UAVs) motivates the development of more efficient aircraft designs. In 2013, we proposed a new quadrotor configuration that uses a single central rotor to provide lift, with small outboard rotors used for attitude control and counter-torque — a triangular quadrotor, or "tri-quad" (see Figs. 1 and 2) [Driessens and Pounds, 2013]. While this configuration demonstrated a 15 per cent improvement in flight energetics compared with a near-identical conventional quadrotor, it also exhibited a precession effect attributed to the gyroscopics of the main rotor. Feedback linearisation control was proposed to correct this effect, but its effectiveness was not assessed.

The gyroscopics problem is not new to aerial robot control. Early quadrotor dynamic models included them as an important contribution to the moments acting on the system [Pounds *et al*, 2002; Hamel *et al*, 2002; Guenard *et al*, 2005]. Individually the gyroscopic moments developed may be quite substantial, and airframes must be sufficiently robust to withstand dynamic rotor loading — gyroscopic torques were strong enough to break the weakly-built arms of an early quadrotor [Pounds *et al*, 2002]. In hovering flight, however, the gyroscopic moments of matched pairs of rotors largely cancel out, and the cumulative torque on the aircraft is small. Some modern textbook dynamical descriptions of quadrotors omit the gyroscopic effects entirely [Corke, 2011]. In the case of a triangular quadrotor where one single large rotor comprises the majority of angular momentum, the gyroscopic moments do not cancel and have a substantial effect on flight attitude [Driessens and Pounds, 2013].

Conventional helicopters resolve the effect of a single main rotor's gyroscopics through the use of flapping hinges [Prouty, 2002, p446]. Flapping hinges are mechanical pivots or flexures that allow rotor blades to pivot up and down about the rotor head (see Fig. 3). By allowing the rotor blade aerodynamic, gyroscopic, weight and centripetal force moments to dynamically balance, the blades will reach a passive equilibrium [Prouty, 2002, p463]; a "see-saw" teetering hinge does not directly transmit flapping torques to the airframe [Pounds *et al*, 2010]. While it is desirable to retain the quadrotor's simplicity of only four moving parts, rotor flapping is a

*Corresponding author

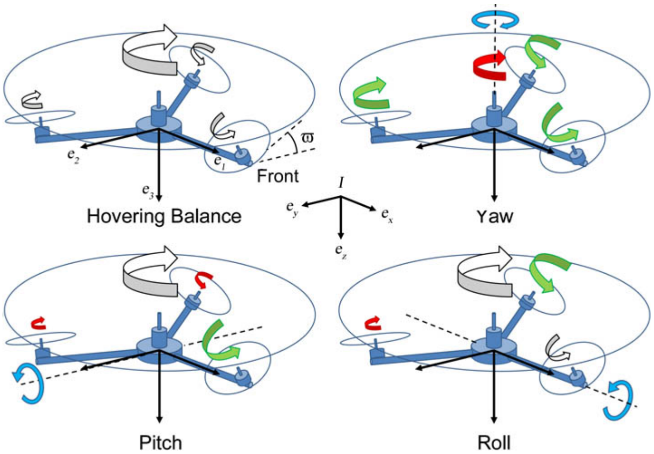

Figure 2: Triangular Quadrotor Manoeuvering Controls. Arrow sizes indicate relative rotor velocities (white arrows are constant).

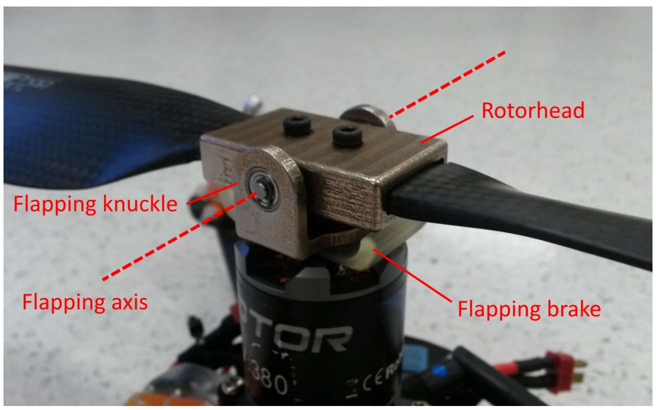

Figure 3: Triangular Quadrotor Flapping Hinge.

viable technique for solving the problem of gyroscopics, at the cost of slightly increased mechanical and dynamic complexity.

In this paper we consider the attitude stability problem for a triangular quadrotor and two methods for compensating for gyroscopic effects. In Section 2 we present simulations of a triangular quadrotor with the previously proposed feedback linearisation control, and observe that system delay makes exact cancellation of gyroscopics impossible. In Section 3 we describe a dynamic model of a triangular quadrotor with a mechanical flapping hinge and present a stabilising controller and simulation of its dynamic response. In Section 4 we report flight experiments of a triangular quadrotor equipped with a teetering flapping hinge. A brief conclusion completes the paper.

2 Feedback Linearisation

It is thought that gyroscopic forces play a substantial role in the flight dynamics of triangular quadrotors. The

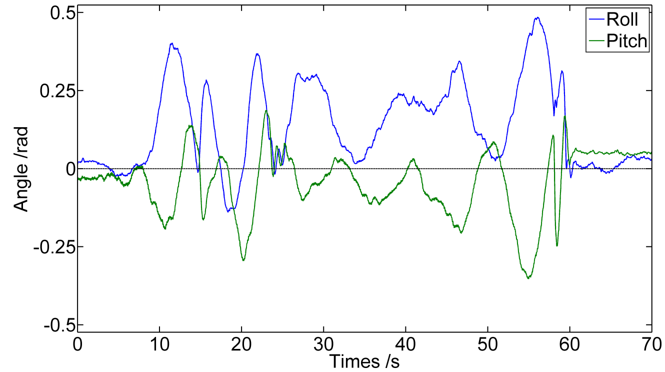

Figure 4: Oscillation of a Triangular Quadrotor With Rigid Rotor in Hovering Flight.

proof of concept Y-4 flown in hover with a rigid main rotor exhibits a large precession (see Fig. 4). A feedback linearisation method was proposed for addressing the problem [Driessens and Pounds, 2013]. However, this work stopped short of implementing the proposed controller; flight tests were conducted without correction factors. In this section, we reprise the dynamic model of a triangular quadrotor with a rigid main rotor and the proposed feedback linearised controller, and present simulations of its motion with and without correction.

2.1 Dynamic Model

The triangular quadrotor rigid rotor dynamic model expressed in the body-fixed frame is:

$$\dot{\boldsymbol{\xi}} = R\boldsymbol{v} \tag{1}$$

$$m\dot{\boldsymbol{v}} = -m\boldsymbol{\Omega}_\times \boldsymbol{v} + mgR'\boldsymbol{e}_3 + T\boldsymbol{e}_3 \tag{2}$$

$$\dot{R} = R\boldsymbol{\Omega}_\times \tag{3}$$

$$\mathrm{I}\dot{\boldsymbol{\Omega}} = -\boldsymbol{\Omega}_\times \mathrm{I}\boldsymbol{\Omega} - \boldsymbol{\Omega}_\times \sum \mathrm{I}_M \boldsymbol{\omega}_M + \boldsymbol{\Gamma} \tag{4}$$

where ξ is the aircraft position, R is the attitude rotation matrix, $\boldsymbol{v}$ is the body velocity, $\boldsymbol{\Omega}$ is the rigid body rotational velocity vector, m and I are the mass and rotational inertia matrix of the flyer, g is acceleration due to gravity and T and $\boldsymbol{\Gamma}$ are the total rotor thrust and torque vectors. The gyroscopic torque function of Ω and the product of the main rotor rotational inertia I_M and angular velocity ω_M.

For simple rotor models, $T_i = \alpha_i \omega_i^2$ and $Q_i = \kappa_i \omega_i^2$, where Q is the induced rotor drag torque.

The force-torque mappings of the rotors are dependent on ϖ, the boom rotor cant angle:

$$\begin{bmatrix}\Gamma_1\\ \Gamma_2\\ \Gamma_3\\ T\end{bmatrix} = \begin{pmatrix} 0 & -\frac{\sqrt{3}}{2}r\alpha C_\varpi & \frac{\sqrt{3}}{2}r\alpha C_\varpi & 0\\ r\alpha C_\varpi & -\frac{1}{2}r\alpha C_\varpi & -\frac{1}{2}r\alpha C_\varpi & 0\\ r\alpha S_\varpi + \kappa C_\varpi & r\alpha S_\varpi + \kappa C_\varpi & r\alpha S_\varpi + \kappa C_\varpi & -\kappa_M\\ \alpha C_\varpi & \alpha C_\varpi & \alpha C_\varpi & \alpha_M \end{pmatrix} \begin{bmatrix}\omega_1^2\\ \omega_2^2\\ \omega_3^2\\ \omega_M^2\end{bmatrix} \tag{5}$$

where α and κ and α_M and κ_M are the boom rotor and main rotor proportional thrust and drag coefficients, respectively. The shorthands S_x and C_x stand for $\sin(x)$ and $\cos(x)$, respectively. If the value of κ is particularly high, ϖ may be low, or even zero.

The gyroscopic torques are almost entirely concentrated in the main rotor — we explicitly ignore the contribution of the smaller rotor gyroscopics. Also explicitly ignored are the small side forces produced by the boom rotors; T incorporates only vertical force contributions.

2.2 Controller

Aside from the different rotor mixing matrix and added gyroscopic term, these dynamics are identical to those of conventional quadrotors — for which highly mature control methods have been developed. It is desirable to employ these same flight controllers with minimal modification to also regulate flight of triangular quadrotors. The proposed attitude control law to correct gyroscopic effects takes the form of a modified conventional linear SISO PID control with gyroscopic cross-coupling cancellation [Driessens and Pounds, 2013]:

$$\Gamma = \left(k_p + k_i\frac{1}{s} + k_d s\right)\begin{bmatrix}\phi\\ \theta\\ \psi\end{bmatrix} - \omega_M \mathrm{I}_{Mzz}\begin{bmatrix}0 & s & 0\\ -s & 0 & 0\\ 0 & 0 & 0\end{bmatrix}\begin{bmatrix}\phi\\ \theta\\ \psi\end{bmatrix} \tag{6}$$

where ϕ, θ and ψ are the roll, pitch and yaw angles of the craft, and k_p, k_i and k_d are control gains identical to those of a standard quadrotor of the same size, weight and boom arm length. With perfect feedback cancellation, the gyroscopic effect would be completely nullified and the dynamics would be identical to an ideal quadrotor.

A key consideration of this controller is the timely generation of control torques that closely cancel the gyroscopic moments. Phase error in the feedback cancellation not only allows the persistence of energy in the gyroscopic precession, but injects additional energy into the motion. The fast rotor speeds and relatively high rotational inertia of the main rotor make strong gyroscopic torques likely; combined with out of phase control torque inputs, even small delays may be destabilising. Potential sources of phase error include the transport delay of inertial measurement unit angular rate sensor measurements and the time response of the boom rotors. Anticipated delays should not compromise the controller.

2.3 Simulation

The dynamics and controller were implemented in a multirotor flight simulator by the authors, available in the Matlab Robotics Toolbox [Corke, 2011], modified for the Y-4 configuration (see Fig. 5). Simulation aircraft parameters were those of the Y-4 testbed [Driessens and Pounds, 2013]. The simulation implements PD attitude control with constant throttle trim, neglecting attitude integral gain or position feedback. The simulator uses a Bogacki-Shampine solver with a fixed time-step of 0.01 seconds. The aircraft's initial conditions are:

$$\xi_0 = [00-0.75]' \tag{7}$$
$$R_0 = I \tag{8}$$
$$v_0 = [000]' \tag{9}$$
$$\Omega_0 = [00.50]' \tag{10}$$

Three simulations were run under PD control: the aircraft without gyroscopic feedback cancellation; the aircraft with 'fastest' gyroscopic feedback cancellation[1]; and the aircraft with feedback with an added 0.01 second delay in angular rotation measurement. In all simulations, the control parameters were $k_p = 0.1$ and $k_d = 0.1$ for both roll and pitch and $k_p = 1$ and $k_d = 1$ for yaw.

Without feedback cancellation the aircraft exhibits initial transients and then a precession effect in pitch and roll like that previously observed experimentally (see Fig. 6). The simulation precession has a much lower amplitude and longer period than that observed experimentally: ± 0.01 rads (approximately ± 0.5 degrees) with a period of approximately 18, compared with ± 0.25 rads (approximately ± 14 degrees) and a period of 10 seconds (see Fig. 4).

The difference in amplitude between the simulated and measured behaviours is substantial. This may be due to errors in the modelled values of rotor and vehicle inertia, or may represent the effect of constant excitation of the precession mode due to outdoor wind. If other physical factors are the cause, then the supposition that gyroscopics are the source of the problem may be wrong. While the disagreement means that absolute conclusions based on the simulations cannot be drawn, we use the simulations results to gain insight into the effectiveness of control designs.

With fastest cancellation the aircraft's roll and pitch velocities are directly fed back into the control loop as a feedforward correction term; this happens with the smallest delay possible in the simulation environment. The precession is reduced in magnitude and frequency to 0.004 rads and 0.0392 Hz (period of 25.5 seconds), and the high frequency transient is shorter (see Fig. 7). It is expected that as the simulation time step approaches zero that the observed precession would trend to zero.

When 0.01 seconds additional delay is introduced to the system, the precession oscillations rapidly grow and

[1] Here fastest feedback is the case where the minimum delay achievable in the simulation is used: one simulation 'tick'.

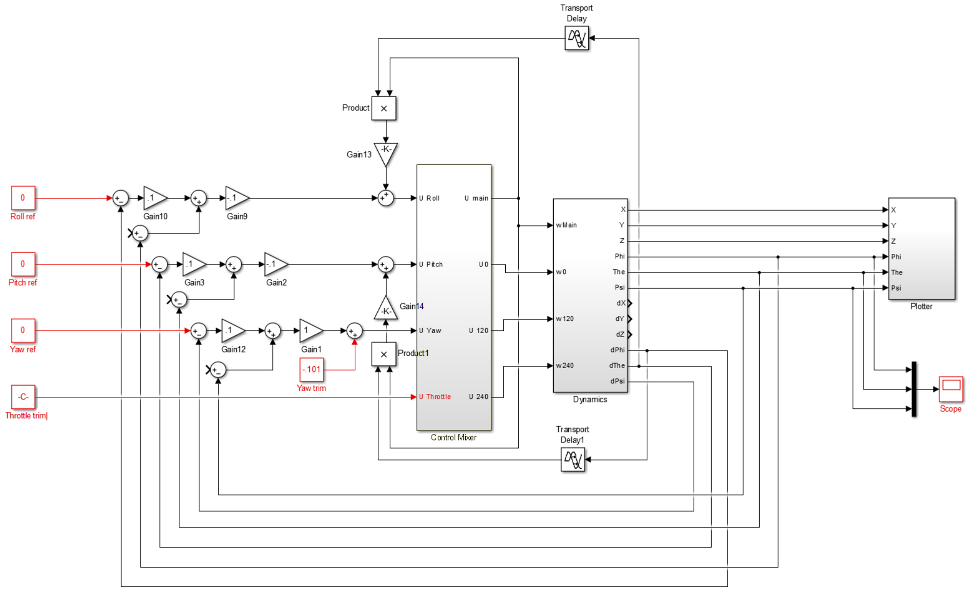

Figure 5: Triangular Quadrotor Flight Dynamics Simulator.

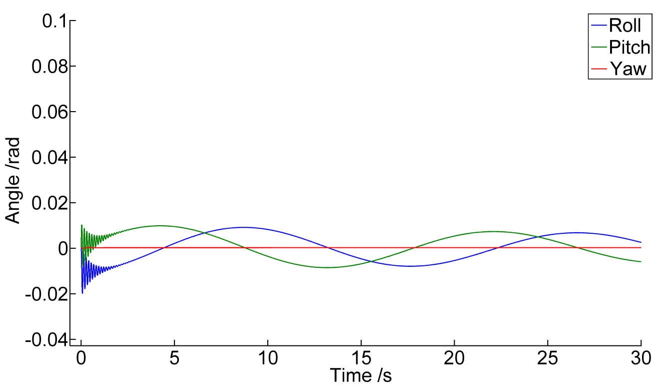

Figure 6: Simulated Pitch Response With Gyroscopic Precession.

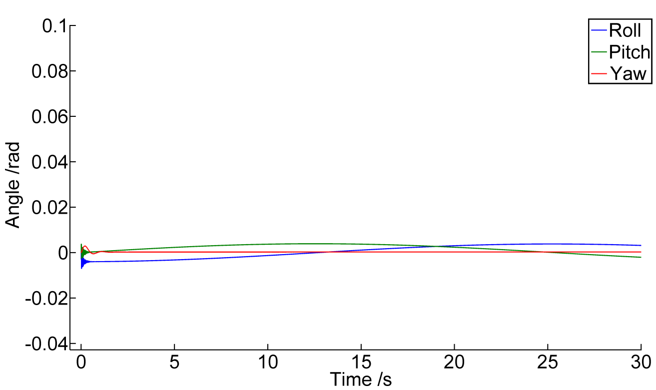

Figure 7: Simulated Feedback Linearisation Pitch Response Without Delay.

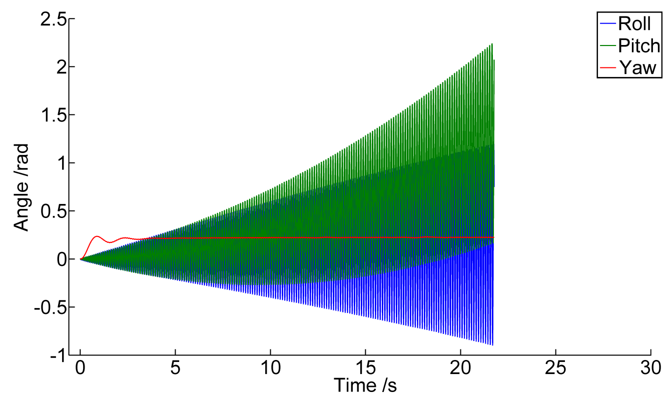

Figure 8: Simulated Feedback Linearisation Pitch Response With 0.01 s Delay.

tracking error is induced in yaw (see Fig. 8[2]). The oscillation mean diverges from level and after 21 seconds the aircraft crashes into the ground and the simulation terminates.

The sensitivity of the gyroscopic system to delay suggests that implementing this control design may not be successful, where even longer delays could be expected in practice. Consequently, we abandoned this approach and instead explored rotor flapping as a potential solution.

3 Flapping Rotor

Adding a flapping joint to the rotor head partially decouples the gyroscopic motion of the rotor from the motion

[2]Note that vertical axis of this graph is scaled differently to Figures 6, 7 and 9.

of the body. Instead, the airframe and rotor's motions are linked by the mechanically fixed angle of attack of the rotor blades as they align with the axis of flapping. This section presents a dynamic model of a triangular quadrotor with flapping and simulations of the system with PD control.

3.1 Dynamic Model

The aerodynamics and modelling of a small-scale rotorcraft are well understood; the following dynamic analysis is substantially based on the author's previous work modelling flapping rotors [Pounds *et al*, 2010; Pounds and Dollar, 2011]

The system dynamic equations are:

$$\dot{\boldsymbol{\xi}} = R\boldsymbol{v} \tag{11}$$

$$m\dot{\boldsymbol{v}} = -m\boldsymbol{\Omega}_\times \boldsymbol{v} + mgR'\boldsymbol{e}_3 + \boldsymbol{T}_M \tag{12}$$

$$\dot{R} = R\boldsymbol{\Omega}_\times \tag{13}$$

$$\mathbf{I}\dot{\boldsymbol{\Omega}} = -\boldsymbol{\Omega}_\times \mathbf{I}\boldsymbol{\Omega} + \boldsymbol{\Gamma} \tag{14}$$

The torque mappings of the rotors are the same as before and once again, we explicitly ignore small side forces produced by the boom rotors. However, the direction of thrust produced by the main rotor will change as the quadrotor manoeuvres. In horizontal motion, on-coming wind causes an imbalance in lift between the blades on each side of the rotor disc. This causes the rotor plane to pitch upward, changing the angle of attack of each blade until a new equilibrium is reached. Likewise, as the aircraft pitches or rolls, the rotor will remain instantaneously unmoved due to gyroscopic stability, resulting in a flapping angle relative to the tilted rotor mast. The angled rotor directs some of its thrust aft, slowing the quadrotor and producing a pitching moment. The rotor flap response is extremely fast, and so it can be represented analytically, without need for additional states.

At low speeds, the flapping angle, β, produced by a zero flapping hinge-offset rotor head is an approximately linear combination of the longitudinal translation and pitch velocities:

$$\beta = q_1\dot{x} - q_2\dot{\theta} \tag{15}$$

where q_1 and q_2 are constant parameters of the rotor [Pounds *et al*, 2010]. This can be extended to 6-DOF by including the lateral components of flapping and abstracting the distortion of the rotor tip plane to include arbitrary velocities [Pounds and Dollar, 2011]:

$$\mathbf{T}_M = -\alpha_M\omega_M^2\Big(I - (Q_1\mathbf{v}_\times\mathbf{e}_3)_\times - (Q_2\boldsymbol{\Omega})_\times\Big)\mathbf{e}_3 \tag{16}$$

where I is the 3×3 identity matrix. Matrices Q_1 and Q_2 are constant translation and rotation flapping parameters of the rotor, respectively:

$$Q_1 = q_1(\mathbf{e}_1 \;\; \mathbf{e}_2 \;\; 0) \tag{17}$$

$$Q_2 = q_2(\mathbf{e}_1 \;\; \mathbf{e}_2 \;\; 0) + \tfrac{1}{\omega_M}(\mathbf{e}_2 \;\; \mathbf{e}_1 \;\; 0) \tag{18}$$

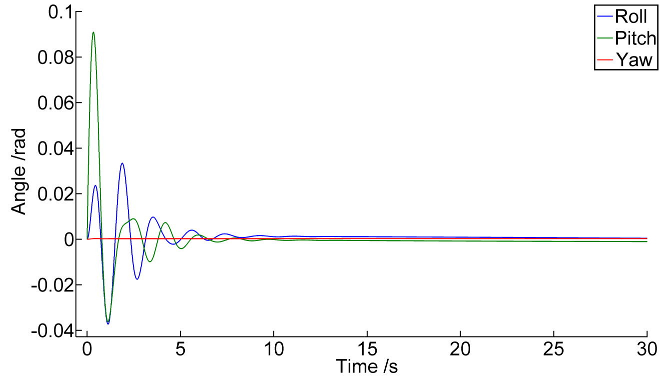

Figure 9: Simulated Flapping Rotor Pitch Response.

The combined dynamics of equations 11–14 are the same as those of a helicopter with zero cyclic input, but with the added pure torque generation capability of a conventional quadrotor. This makes the control task a simple case of applying existing cyclic helicopter control; the boom rotors is analogous to 120° cyclic actuators. In hovering flight, this system can be controlled by a simple SISO PD regulator:

$$\Gamma = \left(k_p + k_i\frac{1}{s} + k_d s\right)\begin{bmatrix}\phi\\ \theta\\ \psi\end{bmatrix} \tag{19}$$

3.2 Simulation

The gyroscopic rotor simulator of Section 2 is easily adapted to represent the mechanics of a quadrotor equipped with a flapping hinge. The same simulation configuration, controller parameters and initial conditions as previously were used to generate the output of the aircraft with a flapping rotor (see Fig. 9). Although the initial transients were larger, the system settled within 15 seconds and decayed to zero. There was no preservation of energy in precession.

4 Experiments

To determine the effectiveness of the flapping hinge in practice, the proof of concept Y-4 aircraft was retrofitted with a flapping rotor assembly. The rotor used was Tiger Motor 18x6.1 carbon fibre rotor, fitted to a 3D printed flapping rotorhead. The rotorhead pivots on two ball race bearings embedded in the flapping knuckle (see Fig. 3). The carbon fibre props are heavier than the adapted 450-series high aspect ratio blades used in previous experiments. For a rigid assembly the gyroscopics of the new rotor would be stronger. Upgrades to the aircraft also include replacement of the Afroflight Naze32 control board with a Pixhawk autopilot and the addition of a telemetry downlink and a second 3-cell 2100 mAh lithium polymer battery. These make the aircraft 200 g heavier than before, for a total mass of 1.1 kg.

Figure 10: Triangular Quadrotor With Flapping Rotor Hovering in Ground Effect.

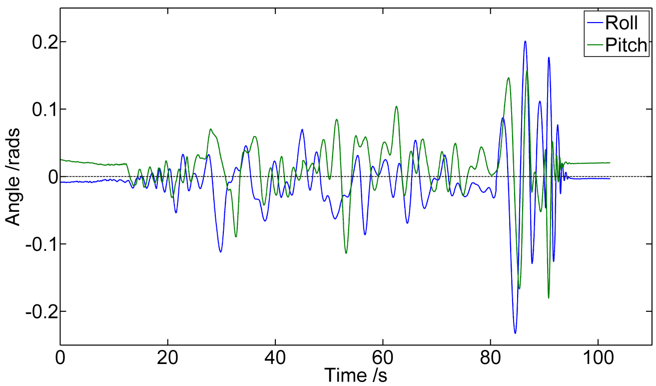

Figure 11: Triangular Quadrotor Pitch and Roll Regulation in Indoor Hovering Flight.

Previous PD pitch and roll control gains implemented in the Naze32 software were $k_p = 2$ and $k_d = 20$. However, it is not clear how these numbers are converted into engineering units for comparison with the Pixhawk controller. Likewise, Pixhawk gains represent a scaling against the maximum thrust range of the motor used, and so vary from model to model. Through empirical testing, the default Pixhawk control gains were found to be effective for the Y-4: $k_p = 7$ and $k_d = 0.1$.

The Y-4 was flown indoors in ground effect to validate the functionality of the attitude controller for the new rotor configuration (see Fig. 10). The response of the aircraft was smooth, and without visible precession (see Fig. 11). At 80 seconds into the flight, the pilot adjusted the yaw trim and manoeuvred the aircraft back to the centre of the testing area, and landed the aircraft at 88 seconds. During free flight, the aircraft maintained level trim (with fixed offsets) within ± 0.114 rads (approximately ± 6.5 degrees) — an improvement over previous performance. This amount of tracking error is still quite high compared with conventional quadrotors, which regularly achieve sub-degree level tracking, but fine-tuning of gains may improve this.

4.1 Limitations and Future Directions

While the flapping-hinge equipped triangular quadrotor does hover stably without precession, as predicted, there are several weaknesses of the current work:

- The simulation analysis that motivates the use of a flapping hinge does not quantitatively reproduce the degree of oscillation observed in experiments.
- The flapping-hinge equipped aircraft exhibits relatively large tracking error from level trim.
- The physical meaning of gains in various attitude controllers is not known, making quantitative comparison difficult.

While the simulator framework has been previously validated, the difference between expected rigid-rotor Y-4 performance and experiment raises questions about the model's implicit assumptions. The rigid-rotor tests were conducted outside, as opposed to the ideal still-air assumed by the simulator.

It is thought that the experimental tracking error is due to untuned gain and flying close to the ground in an indoor environment, which can induce oscillations in multirotors due to differential ground effect. It is also possible that during flapping the pivoting rotor tip comes close to the boom rotors and may interact in a manner not seen in the fixed rotor format. Furthermore, the indoor experiments were conducted in a small room, allow recirculation of the rotor outflows, which can lead to reingestion of turbulence.

Thus, the next step of this work will be to undertake test flights in a large indoor arena. For better comparison, we will then convert the current hardware back to the fixed-pitch configuration using the Pixhawk controller to conduct reference flights. This will allow us to establish a clear baseline for precession behaviour and make direct comparison with equal control gains.

5 Conclusions

This paper explored two methods for addressing the problem of rotor gyroscopics for a new type of triangular quadrotor. Simulations suggested that the previously proposed approach — feedback linearisation — would not be successful. However, these simulations were not decisive, due to differences in the amplitude of the computed output and experimental measurements. On the basis of these simulations, we instead opted to use a flapping hinge to obviate the need for gyroscopic corrections. This system proved to be successful both in simulation and experiment. Although the system works, uncertainties about the source of precession and in the way gains are implemented in commercial flight controllers used makes comparison between the two approaches difficult. Ongoing work will include more comparative experiments to establish a baseline.

6 Acknowledgements

The authors would like to thank Craig Freakley and Dion Gonano for their assistance with this work.

References

[Driessens and Pounds, 2013] S. Driessens and P. Pounds, "Towards and More Efficient Quadrotor Configuration," In Proc. IEEE/RSJ International Conference on Intelligent Robots and Systems, 2013.

[Pounds *et al*, 2002] P. Pounds, R. Mahony, P. Hynes and J. Roberts, "Design of a Four-Rotor Aerial Robot", In Proc. of Australasian Conference on Robotics and Automation, 2002.

[Hamel *et al*, 2002] T. Hamel, R. Mahony, R. Lozano and J. Ostrowski, "Dynamic Modelling and Configuration Stabilization for an X4-Flyer", In Proc. 15th Triennial World Congress of the International Federation of Automatic Control, 2002.

[Guenard *et al*, 2005] N. Guenard, T. Hamel and V. Moreau, "Dynamic Modeling and Intuitive Control Strategy for an 'X4-Flyer". In Proc. International Conference on Control and Automation, 2005.

[Corke, 2011] P. Corke, Robotics, Vision and Control, Springer Science & Business Media, Springer Tracts in Advanced Robotics, Vol. 73, 2011.

[Prouty, 2002] R. Prouty, Helicopter Performance Stability and Control, Krieg Publishing Company, 2002.

[Pounds *et al*, 2010] P. Pounds, P. Corke and R. Mahony, "Modelling and Control of a Large Quadrotor Robot," Control Engineering Practice, Vol. 18, No. 7, pp 691-699, 2010.

[Pounds and Dollar, 2011] P. Pounds and A. Dollar, "UAV Rotorcraft in Compliant Contact: Stability Analysis and Simulation," In Proc. IEEE/RSJ International Conference on Intelligent Robots and Systems, 2011.

[Leishman, 2006] J. G. Leishman, Principles of Helicopter Aerodynamics, 2nd Ed., Cambridge University Press, New York, 2006.